Journal of King Saud University – Science 32 (2020) 21–28

Contents lists available at ScienceDirect

Journal of King Saud University – Science

journal homepage: www.sciencedirect.com

Original article

Tribological properties of aluminium-clay composites for brake disc rotor applications

A.A. Agbeleye [a,b,*], D.E. Esezobor [a], S.A. Balogun [a], J.O. Agunsoye [a], J. Solis [b], A. Neville [b]

[a] Metallurgical and Materials Engineering Department, University of Lagos, Lagos, Nigeria
[b] Institute of Functional Surfaces, School of Mechanical Engineering, University of Leeds, Leeds, UK

ARTICLE INFO

Article history:
Received 14 August 2017
Accepted 7 September 2017
Available online 8 September 2017

Keywords:
Sliding wear
Surface analysis
Sliding friction
Hardness
Three-body abrasion

ABSTRACT

In this paper, the mechanical and tribological behaviours of various compositions of aluminium 6063 alloy – clay (Al-clay) composites for brake pad applications were studied. The Al-clay composites with 5–30 wt% of clay particles of grain size of 60 BSS (250 microns) were developed through stir casting route. The wear characteristics of Al-clay in dry sliding conditions were subjected to a series of Denison T62 HS pin-on-disc wear tests. The action of two different loads (4 and 10 N), three sliding speeds of 200, 500 and 1000 rpm were investigated. The results of the mechanical and wear tests as well as the metallographic investigation of optical, scanning electron microscopy and energy dispersive X-ray microscopy revealed an improvement in the tensile strength, hardness and wear resistance in the composites with 10–25 wt% clays. The best values were obtained at 15 wt%. Wear rate was highly influenced by applied load and sliding speed. The developed composites with 15–25 wt% clay addition were similar to conventional semi metallic brake pad in terms of wear and friction properties.
© 2017 Production and hosting by Elsevier B.V. on behalf of King Saud University. This is an open access article under the CC BY-NC-ND license (http://creativecommons.org/licenses/by-nc-nd/4.0/).

1. Introduction

Aluminium based composites are gaining increased applications in the transport, aerospace, marine, oil and gas, automobile and mineral processing industries, due to their excellent strength, stiffness and wear resistance properties. However, their widespread adoption for engineering applications has been hindered by the high cost of producing components (Burkinshaw et al., 2012). Hence much effort has been geared toward the development of composites with reinforcements that are relatively cheap and can compete favourably in terms of strength and wear characteristics with composites reinforced with silicon carbide (SiC), aluminium oxide (Al_2O_3) and graphite. Clay could be a potential reinforcing component due to its availability and its major constituents such as alumina (Al_2O_3), silica (SiO_2), oxides of iron (Fe_2O_3), titanium (TiO_2), and sodium (Na_2O).

Recently, great interest has been in the automobile and aviation industries and many other industries to reduce strength-to-weight ratio of components, improve the wear resistance of components, and or enhance fuel efficiency as evidenced by extensive research into aluminium-based composites (Rao et al., 2009; Rawal, 2001; Das, 2004). One of such area being considered for potential weight reduction is the brake system. Most cars today are built with disc brake which consists of the caliper and a ventilated rotor. The caliper and rotor are typically made from ductile cast iron and grey cast iron respectively. Cast aluminium and aluminium based metal matrix composites (MMC) brake rotors give as much as 45–61% weight reduction in the braking system (Sarip and Day, 2015; Huang and Paxton, 1998; Macke and Rohatgi, 2012; Miracle and Donaldson, 2001; Maleque et al., 2010). However, the major limitation of the use of aluminium alloys is its soft nature, hence the need for its reinforcement with high strength-stiffness materials such as SiC, TiC, TiB_2, B_4C, Al_2O_3, and Si_3N_4 (Jimoh et al., 2012). Clay contains reinforcing materials such as Al_2O_3, SiO_2 and Fe_2O_3 with trace presence of other materials (Esezobor et al., 2014) making it a potential candidate as a reinforcing agent for the production of metal matrix composite for wear applications. Wear is one of the most commonly encountered industrial problems that leads to the replacement of components and assemblies in engineering. When two solid surfaces are placed in solid-state contact, it is not easy to envision the absence of some wear even in the most

* Corresponding author at: Metallurgical and Materials Engineering Department, University of Lagos, Lagos, Nigeria.
E-mail address: aagbeleye@unilag.edu.ng (A.A. Agbeleye).
Peer review under responsibility of King Saud University.

Production and hosting by Elsevier

http://dx.doi.org/10.1016/j.jksus.2017.09.002
1018-3647/© 2017 Production and hosting by Elsevier B.V. on behalf of King Saud University.
This is an open access article under the CC BY-NC-ND license (http://creativecommons.org/licenses/by-nc-nd/4.0/).

efficiently lubricated systems because of asperity contact (Narayanasamy and Selvakumar, 2016).

During the sliding action, the hard ceramic particles detached from the composite surface constitute a resisting barrier in reducing the wear rate of the composite material. The sliding wear resistance of the composites with respect to that of alloy varies with the process parameters (Al-Qutub, 2009; Alpas and Zhang, 1993; Balakumar, 2013). The three distinct regions of wear reported by Alpas and Zhang, 1993 are dependent of load, which include oxidative wear in which the oxide aluminium surface layer is removed during sliding process. Other regions include the mild wear in which the loss of material is dictated by asperity-to-asperity contact and the wear that is controlled essentially by subsurface deformation and fracturing of the surface (Suh and Saka, 1980). These regions occur at low, medium and high load regimes.

The braking system of a vehicle is usually subjected to a complex state of stress which includes mechanical and thermal stresses (Choudhury et al., 2014). The material used in brake rotors should, therefore be able to bear thermal fatigue and should absorb and quickly dissipate heat generated during braking (Esposito and Thrower, 1999). In a typical braking process, the hydraulic pressure could be in the range of 2 to 4 MPa. The rotors could reach at a very small duration, temperatures as high as 800 °C due to friction, which could result to a thermal gradient up to 500 °C between the surface and the core of the rotors (Macnaughta, 1998).

Friction materials for brake systems comprise metallic components to improve their wear resistance, thermal stability and strength. Metals such as copper, steel, iron, brass, bronze, and aluminium have been used in the form of fibres or particles in the friction materials. The friction and wear of these materials depend mainly on the type, morphology, and hardness of the metallic ingredients (Jang et al., 2004). A commercial brake lining usually contains more than 10 different constituents categorized into four classes of ingredients: binders, fillers, friction modifiers and reinforcements. The choice of the constituents is often based on individual experience or a trial and error method to make a new formulation (Hee and Filip, 2005).

The incorporation of clay particles in aluminium alloy will harness the potential of its constituents (mainly Al_2O_3+SiO_2) forming multi-reinforcements composite with the prospect of it a suitable substitute in wear resistant applications, in place of the monolithic reinforcements such as SiC, Al_2O_3, etc. currently in use.

Therefore, this paper will investigates the influence of various weight fractions of aluminosilicate clay on the mechanical, friction and wear properties of Al-clay composites for brake disc rotor applications. The results will be compared with the results obtained with a semimetallic brake pad (SMBP).

Table 1
Optical Emission Spectrometric analysis of AA6063.

Element	Si	Mg	Fe	Cu	Mn	Zn	Cr	Ti	Al
% composition	0.429	0.425	0.225	0.004	0.026	0.002	0.006	0.033	98.850

Table 2
Atomic Absorption Spectroscopy (AAS) analysis of clay sample.

Parameters	SiO_2	Al_2O_3	Fe_2O_3	MnO	MgO	Na_2O	CaO	K_2O	BaO	SO_3	LOI
Level detected (%)	45.62	33.74	0.43	0.01	0.06	0.05	0.04	0.63	0.01	0.03	4.545

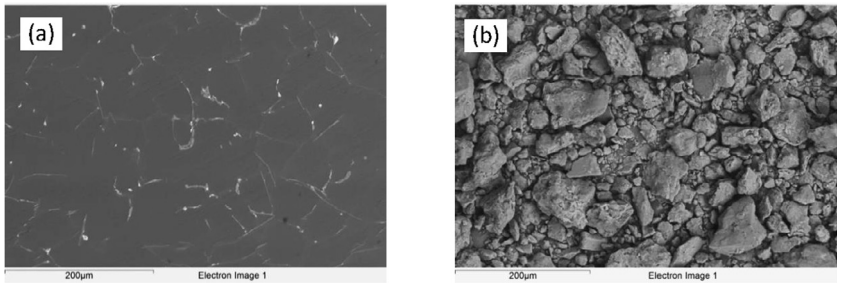

Fig. 1. SEM micrographs of: (a) As - cast AA6063 and (b) Clay particles.

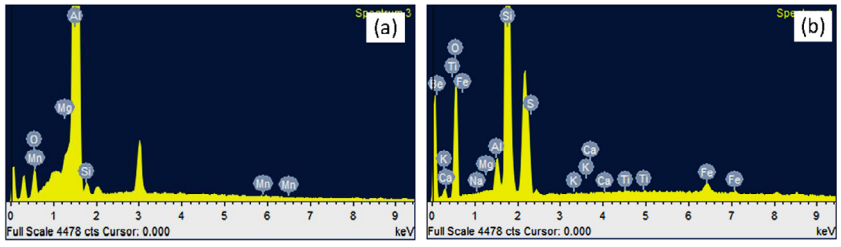

Fig. 2. EDX analysis of (a) As - cast AA6063 and (b) Clay particles.

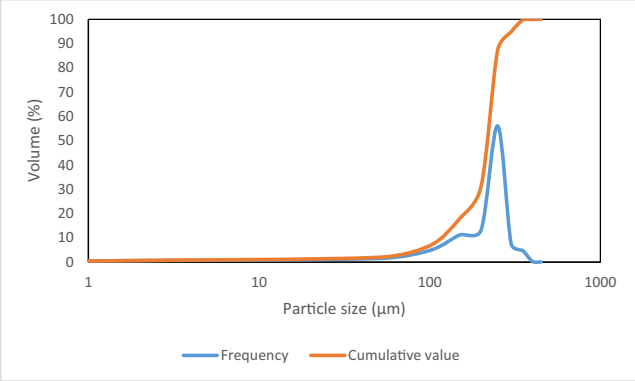

Fig. 3. Particle size distribution of clay sample (Narayanasamy and Selvakumar, 2017).

2. Experimental

The Al-clay composites which consist of aluminium alloy (AA6063) and 5–30 wt% of clay particles of grain size of 60 BSS (250 microns) were developed through liquid metallurgy stir casting route. The AA6063 was supplied by Nigerian Aluminum Extrusion Company (NIGALEX), Oshodi, Lagos, and the clay was obtained from Ikorodu town in Lagos State, Nigeria.

The tensile and Vickers hardness tests of samples were conducted using respectively 50 kN Instron 3369L3477 machine and Mitutoyo micro–hardness tester HM-122 in accordance with the ASTM E8/E8M-13 standards. The Metallographic examination was carried out using Zeiss EVO MA-15 Scanning Electron Microscope (SEM)/Energy Dispersive Xray (EDX). The sample surfaces were ground, polished using alumina suspension, and etched in Weck's reagent for 20 s as well as dried in still air. The microstruc-

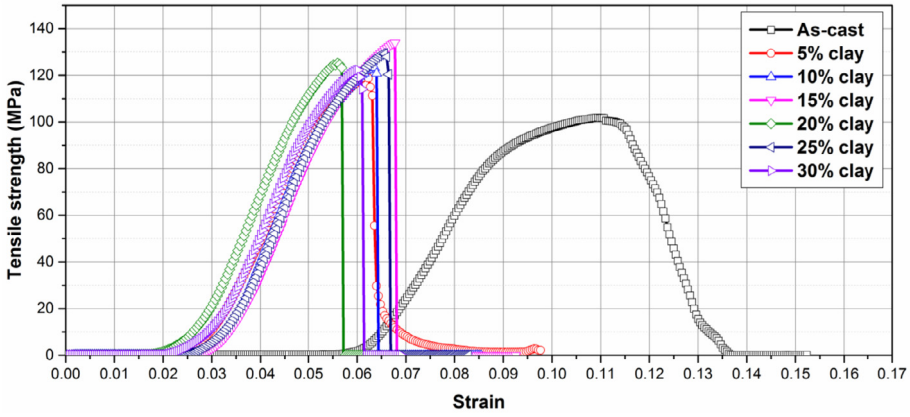

Fig. 4. Tensile strength against strain.

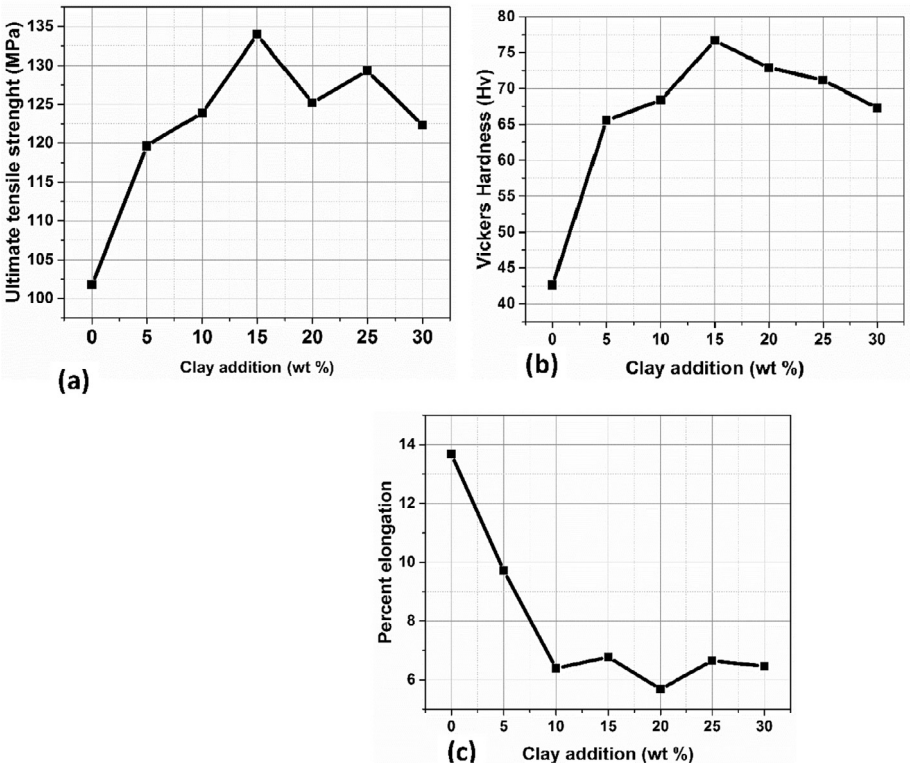

Fig. 5. Mechanical properties of test samples: UTS, (a) Vickers hardness, (b) and Percent elongation, (c).

ture of each samples were also examined with a digital Leica CTR6000 metallurgical microscope at 50 μm magnification.

The wear characteristics of Al-clay and SMBP in dry sliding conditions were subjected to a series of Denison T62 HS pin-on-disc wear tests. Cylindrical pins of 5 mm diameter were made from the Al-Clay composite and SMPD. The action of two different loads (4 and 10 N), on AISI stainless steel disc at three sliding speeds of 1.05, 2.62 and 5.24 m/s were investigated as per ASTM: G99-05 standard. The wear was measured by weighing the pins before and after the test.

The volumetric wear rate was estimated by measuring the mass loss, Δm in the sample after each test. The volumetric wear rate W_r, which relates to the mass loss to the composite density, ρ and the sliding time, t was evaluated using the expression in Eq. (1):

$$W_r = \frac{\Delta m}{\rho t} \tag{1}$$

However, it is more appropriate to express the wear results in terms of wear constant K as extracted from Archard's law. For known values of wear volume V, Vickers hardness H of the softer component, sliding distance S, and normal load L, the wear coefficient is given in Eq. (2):

$$K = \frac{VH}{LS} \tag{2}$$

3. Results

3.1. Mechanical properties

The results of the analysis of the aluminium alloy and the clay are presented in Tables 1 and 2 respectively. Figs. 1 and 2 show the SEM images and the EDX analysis of the AA6063 and clay samples used in this study respectively.

The results of the SEM/EDX (Figs. 1 and 2) revealed the as cast sample contains proportion of Al, Si and Mg in the range expected in AA6063, while clay sample contains the right proportion of Si, Al, Fe, O, Mg, Na, Ca and K that placed it in the range of aluminosilicate clay group as classified by Chesti, 1986. The size distribution of the clay particles is shown in Fig. 3.

The UTS of the composite samples increases as the addition of clay increases to a peak value of 133.98 MPa at 15 wt% clay particle addition over the conventional AA6063 of 104 MPa. Further increase in clay particle addition to 30 wt% clay resulted in a decline in the UTS to 122.29 MPa (Fig. 4).

The Vickers hardness values of the Al-clay composite are presented in Fig. 5. The increase in the percentage of clay particle addition was accompanied with corresponding increase in the hardness values and it reached a maximum value of 76.7 HV at 15 wt% after which the hardness value declined to 67.3 at 30 wt %. The percent elongation (ductility) values of the Al-Clay compos-

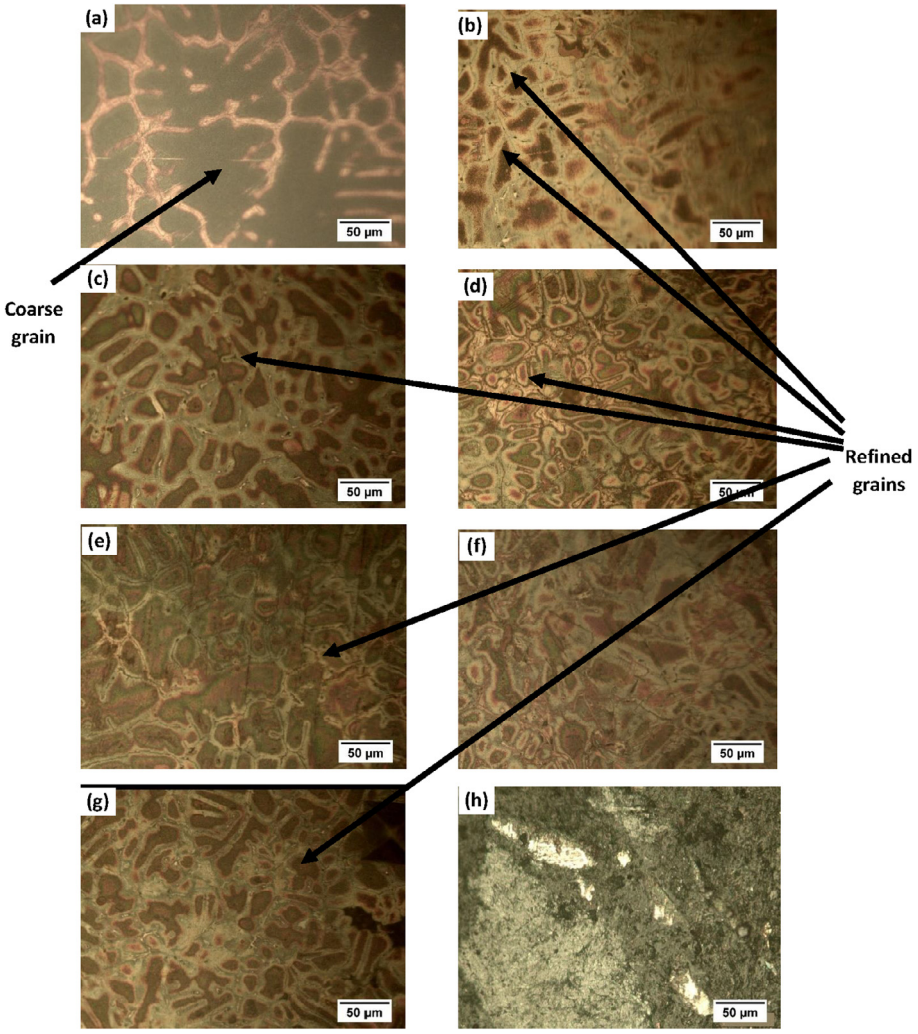

Fig. 6. Optical microstructure of the samples (a) As cast AA6063, (b) 5% clay, (c) 10% clay, (d) 15% clay, (e) 20% clay, (f) 25% clay, (g) 30% clay, (h) SMPB.

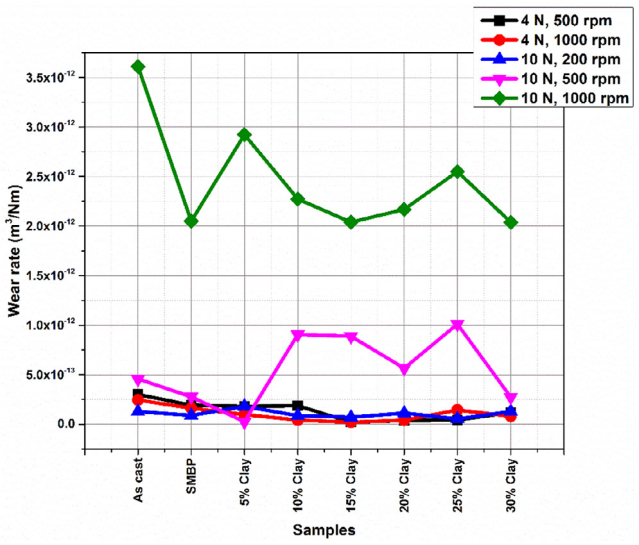

Fig. 7. Dimensional wear coefficient of test samples at varied loads and sliding speeds.

ites as presented in Fig. 5(c) show appreciable response to increase in clay particle addition. Strain values generally decrease with increase in clay particle addition with the minimum value of 5.7% attained at 20 wt.%.

3.2. Microstructure

The results of the metallographic examination of all the samples are displayed in Fig. 6. The clay particles are fairly distributed along the grain boundaries of the AA6063 matrix. The addition of the clay particles is observed to have enhanced the formation of finer grains (Fig. 6(b-h)) as compared to the as-cast AA6063 (control sample) (Fig. 6a).

3.3. Wear characteristics

The result of the wear test of the composites with various weight fractions of clay particles is displayed in Fig. 7.

The wear rate decreases with increase in the weight fraction of the reinforcing agent (clay) as compared to conventional AA6063. The lower wear rate observed at optimum condition between 15–20 wt% clay is due to enhanced hardness by the dispersion of the hard intermetallics over the AA6063 matrix, which acted as load supporting elements (Essam et al., 2010; Devaraju et al., 2013a,b; Kumar and Balasubramanian, 2008).

The wear behaviour of the developed composites is similar to the SMBP at lower sliding speed of 200 rpm for all samples. In some cases, the composites have enhanced wear properties. This behaviour can be attributed to the release of the clay particles on the surface during wear process, which to an extent may prevent metal to metal contact and also serve as solid lubricants (Tjong et al., 1999). On the other hand, the wear rate increases with

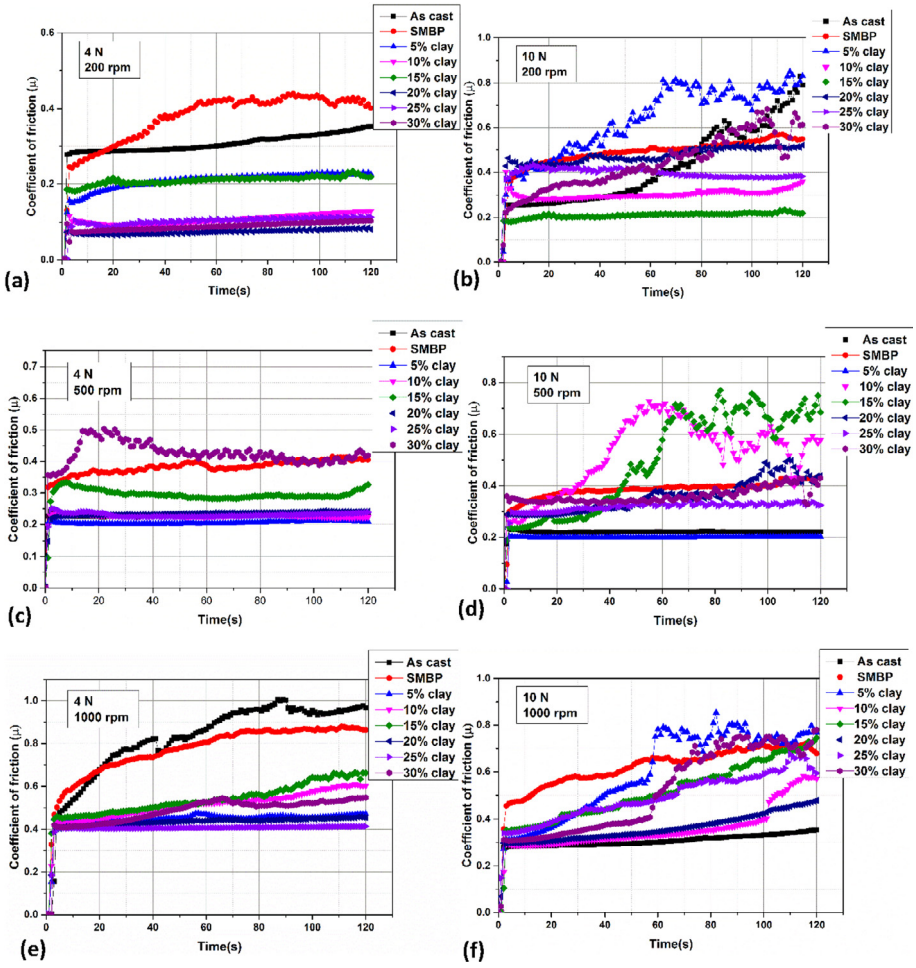

Fig. 8. Coefficient of friction (a) 4 N at 200 rpm, (b) 10 N at 200 rpm, (c) 4 N at 500 rpm, (d) 10 N at 500 rpm, (e) 4 N at 1000 rpm, (f) 10 N at 1000 rpm under ambient and dry conditions.

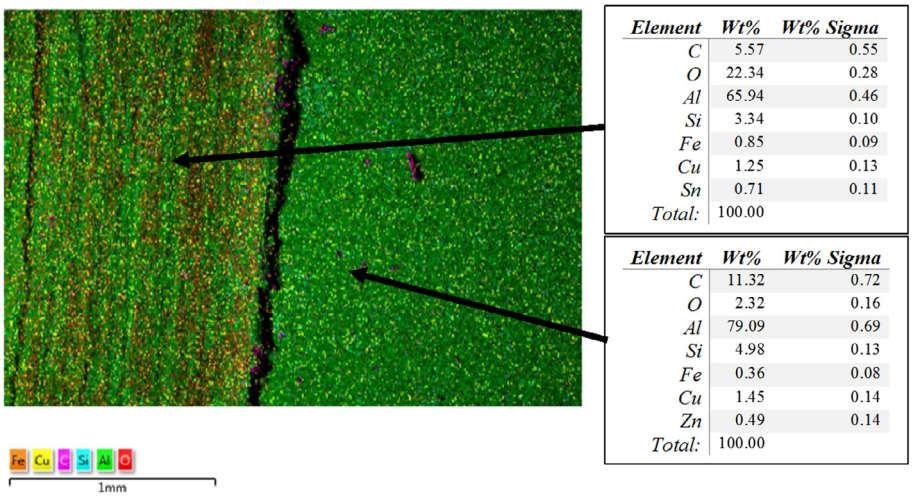

Element	Wt%	Wt% Sigma
C	5.57	0.55
O	22.34	0.28
Al	65.94	0.46
Si	3.34	0.10
Fe	0.85	0.09
Cu	1.25	0.13
Sn	0.71	0.11
Total:	100.00	

Element	Wt%	Wt% Sigma
C	11.32	0.72
O	2.32	0.16
Al	79.09	0.69
Si	4.98	0.13
Fe	0.36	0.08
Cu	1.45	0.14
Zn	0.49	0.14
Total:	100.00	

Fig. 9. EDS layered image of wear track.

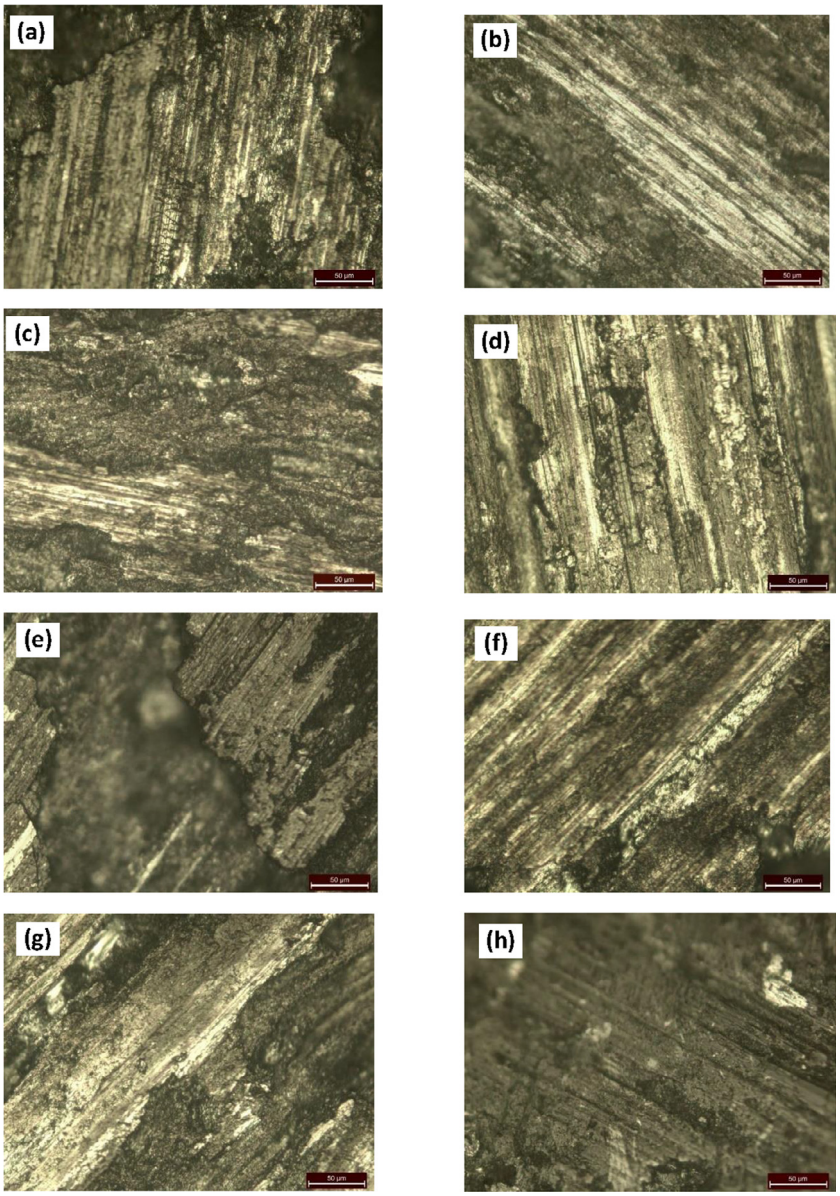

Fig. 10. Optical microstructure of worn surfaces of samples (a) As cast AA6063, (b) 5% clay, (c) 10% clay, (d) 15% clay, (e) 20% clay, (f) 25% clay, (g) 30% clay, (h) SMPB.

increase in the normal load and sliding speed. This trend was also observed in the work of Devaraju et al., 2013b. However 10–25% weight fraction at 10 N and 500 rpm show increase in the wear rate of the composite. This shows the dependence of load and the weight fraction of clay particle on the wear behaviour of the composite over conventional AA6063.

3.4. Friction characteristics

The variation of coefficient of friction (CoF) of the test samples with the sliding time with respect to the various sliding load and the rotating speeds in dry conditions is presented in Fig. 8. It was observed that the CoF increased sharply in the first few seconds and then attained a nearly steady value with the sliding time. The initial high value of the CoF can be attributed to the roughness at the surface of the specimen (Sharma et al., 2012). However, the CoF value increases with increase in load at low rotating speed.

However, at higher speed the average CoF is found to be independent of load during the first few seconds of the experiment. After a while, the amplitude of CoF increases at high load, producing fluctuating values of CoF. This could be due to the presence of higher volume of wear debris trapped at the contact zone creating a third body effect within the contact surface, resulting in decrease in metal removal during the wear test (Devaraju et al., 2013b).

3.5. Worn surface morphology

The morphology of the worn test samples showed in Fig. 10 indicate that there exist three microstructurally distinct areas with the wear tracks. These areas include: bright coloured area with scratches (part of the based metal), light grey areas, and dark grey areas.

The bright coloured area on the micrographs is the uncovered metal surface. This appears smooth, indicative of mild oxidational type of wear with no or minimal cracks. The grey area on the other hand, appear to be consisting of smaller compacted particles and with considerable cracks appearing on the surface. The oxidation of ruptured particle during sliding is called fragmented oxide particle. When this small particles were oxidized and emitted during sliding, they reduced the sliding contact surfaces. The fragmented oxide particle acts as a lubricating agent, and it may reduce wear. Consequently, no plastic deformation will occur on the worn surface of the Al-Clay composite (Narayanasamy and Selvakumar, 2017).

4. Discussion

The improvement of the UTS and microhardness with the increment in the weight fraction of clay particles may be due to the presence and pinning effect of the clay particles (Khraisat and Abu Jadayil, 2010; Essam et al., 2010; Devaraju et al., 2013a,b), which serve as impingement for the movement of dislocations and as a result restrict the sliding of the grain boundaries. The results of the mechanical property tests also indicate that ductility of the AA6063 was influenced by the amount of clay particles addition. This is evident with a decrease in percent elongation, which dropped to its minimum at 20 wt% clay particle addition.

The improved mechanical properties of the composite (Fig. 5) can be attributed to the combined effect of grain refinement propelled by increase in clay content and the formation, precipitation, and distribution of hard intermetallic compounds (Khraisat and Abu Jadayil, 2010). Previous studies (Marioara et al., 2003; Kuijpers et al., 2003; Miao and Laughlin, 1999) have shown that the mechanical properties are highly influenced by the precipitates of hardening β(Mg_2Si) phase. The strength is also influenced by the intermetallic phases formed during solidification of the alloys.

The Compositional variations of wear track as presented in Fig. 9 shows higher oxygen content of tribo-layer. This might be due to presence of oxides of elements (such as Al, Si, Cu, Sn, and Fe) present in the test materials.

Wear debris is attributed to delamination and fatigue wear of tribo-layers. Other sources of debris formation were identified as pin material fractured particles mostly at edges, and formation of third body abrasive particles during the test by tribo-oxidation and mechanical mixing of test products.

5. Conclusions

It can be concluded that:

(i). The addition of clay particles generally improved the mechanical properties, wear resistance and CoF of the AA6063.

(ii). The wear behaviour of the developed composite is dependent on the applied load, sliding speed and the weight fraction of clay particle additive.

(iii). The wear and friction properties of the developed composite with 15–30 wt% clay particles addition are similar to that of SMBP and therefore can be substituted.

(iv). The low wear rate exhibited at the surface of the developed composite occurred as a result of the presence of fractured particles between the composite pin and steel disc surfaces. The particles served as load bearing elements as well as solid lubricant.

References

Alpas, A.T., Zhang, J., 1993. Wear regimes and transitions in Al_2O_3 particulate-reinforced Al alloys. Mater. Sci. Eng. A 161, 273.

Al-Qutub, A.M., 2009. Effect of heat treatment on friction and wear behaviour of Al-6061 composite reinforced 10% submicron Al_2O_3 particles. Arab. J. Sci. Eng. 24, 205–215.

Balakumar, G., 2013. Tensile and wear characterisation of aluminium alloy reinforced with nano-ZrO_2 metal matrix composites (NMMCs). Int. J. Nano Sci. Nanotechnol. 4 (1), 121–129.

Burkinshaw, M., Neville, A., Morina, A., Sutton, M., 2012. Calcium sulphonate and its interactions with ZDDP on both aluminium-silicon and model silicon surfaces. Tribol. Int. 46, 41–51.

Chesti, A.R., 1986. Refractories, Production and Properties. The Iron and Steel Institute, London, p. 3-13, 295-314.

Choudhury, P., Singh, R.K., Panda, P., 2014. Thermal and structural analysis of a ceramic coated Fsae brake rotor using 3D finite element method for wear resistance and design optimisation. IOSR J. Mech. Civ. Eng. 11 (2), 143–149.

Das, S., 2004. Development of aluminium alloy composites for engineering applications. Trans. Indian Inst. Met. 57, 325–334.

Devaraju, A., Kumar, A., Kumsrswamy, A., Kotiveerachari, B., 2013a. Influence of reinforcements (SiC and Al2O3) and rotational speed on wear and mechanical properties of aluminium alloy 6061–T6 based surface hybrid composites produced via friction stir process. Mater. Des. 51, 331–341.

Devaraju, A., Kumar, A., Kumsrswamy, A., Kotiveerachari, B., 2013b. Wear and mechanical properties of 6061–T6 aluminium alloy surface hybrid composites [(SiC+Gr) and (SiC+ Al2O3)] fabricated by friction stir processing. J. Mater. Res. Technol. 2 (4), 362–369.

Esezobor, D.E., Obidiegwu, E.O., Lawal, G.I., 2014. The influence of agro-forestry waste addictive on the thermal insulating properties of Osiele clay. J. Emerg. Trends Eng. Appl. Sci. 5 (5), 305–311.

Esposito, A., Thrower, J., 1999. Machine Design. Delmar Publishers Inc..

Essam, R.I., Makoto, T., Tishiya, S., Kenji, I., 2010. Wear characteristics of surface hybrid MMCs layer fabricated on aluminium plate by friction stir processing. Wear 268, 1111–1121.

Hee, K.W., Filip, P., 2005. Performance of ceramic enhanced phenolic matrix brake lining materials for automotive brake linings. Wear 259, 1088–1096.

Huang, S.X., Paxton, K., 1998. A macro-composite Al brake rotor for reduced weight and improved performance. JOM 50 (8), 26–28.

Jang, H., Koa, K., Kima, S.J., Basch, R.H., Fash, J.W., 2004. The effect of metal fibers on the friction performance of automotive brake friction materials. Wear 256, 406–414.

Jimoh, A., Sigalas, I., Hermann, M., 2012. In Situ synthesis of titanium matrix composite (Ti-TiB-TiC) through sintering of TiH_2-B_4C. Mater. Sci. Appl. 3, 30–35.

Khraisat, W., Abu Jadayil, W., 2010. Strengthening aluminium scrap by alloying with iron. Jordan J. Mech. Ind. Eng. 4 (3), 372–377.
Kuijpers, N.C.W., Kool, W.H., Koenis, P.T.G., Nilsen, K.E., Todd, I., Van der Zwaag, S., 2003. Assessment of different techniques for quantification of α-Al(FeMn)Si and β-AlFeSi intermetallics in AA 6xxx alloys. Mater. Charact. 49, 409–420.
Kumar, S., Balasubramanian, V., 2008. Developing mathematical model to calculate wear rate of AA7075/SiC_p powder metallurgy composite. Wear 264, 1026–1034.
Macke, A., Rohatgi, P., 2012. Metal Matrix Composites offer the automotive industry opportunity to reduce vehicle weight, improve performance. Adv. Mater. Proc. 170 (3), 19–23.
Macnaughta, M., 1998. Cast iron brake discs—a brief history of their development and metallurgy. Technical Report, Foundryman. p. 321.
Maleque, M.A., Dyuti, S., Rahman, M.M., 2010. Materials selection method in design of automotive brake disc. In: Proceedings of the World Congress on Engineering. June 30-July 2; London, UK (vol. 3, ISBN 978-988-18210-8-9).
Marioara, C.D., Andersen, S.J., Jansen, J., Zandbergen, H.W., 2003. The influence of temperature and storage time at RT on nucleation of the β" phase in a 6082 Al-Mg-Si alloy. Acta Mater. 51, 789–796.
Miao, W.F., Laughlin, D.E., 1999. Precipitation hardening in aluminium alloy 6022. Scr. Mater. 40 (7), 873–878.
Miracle, D.B., Donaldson, S.L., 2001. ASM Handbook, Vol. 21: Composites. ASM International, Materials Park, OH.
Narayanasamy, P., Selvakumar, N., 2016. Tensile, compressive and wear behaviour of self-lubricating sintered magnesium based composites. Trans. Nonferrous Met. Soc. China. 27, 312–323.
Narayanasamy, P., Selvakumar, N., 2017. Effect of hybridizing and optimization of tic on the tribological behaviour of mg–mos_2 composites. J. Tribol. 139 (5), 051301–051311.
Rao, R.N., Das, S., Mondal, D.P., Dixit, G., 2009. Dry sliding wear behaviour of cast high strength aluminium alloy (Al–Zn–Mg) and hard particle composites. Wear 267, 1688–1695.
Rawal, R.S., 2001. Metal matrix composites for space applications. JOM 53, 14–17.
Sarip, S., Day, A.J., 2015. An experimental study on prototype lightweight brake disc for regenerative braking. Jurnal Tecknologi (Sci. Eng.) 74 (1), 11–17.
Sharma, N., Kumar, N., Dash, S., Das, C.R., Subba Rao, R.V., Tyagi, A.K., Raj, B., 2012. Scratch resistance and tribological properties of DLC coatings under dry and lubricated conditions. Tribol. Int. 56, 129–140.
Suh, N.P., Saka, N., 1980. In: Suh, N.P., Saka, N. (Eds.), Fundamentals of Tribology. The MIT Press, Cambridge, p. 443.
Tjong, S.C., Lau, K.C., Wu, S.Q., 1999. Wear of Al-based hybrid composites containing BN and SiC particulates. Metall. Mater. Trans. 30A, 2551–2555.